Journal of Statistical Mechanics: Theory and Experiment
An IOP and SISSA journal

Simple shear flow in inelastic Maxwell models

Andrés Santos and Vicente Garzó

Departamento de Física, Universidad de Extremadura, E-06071 Badajoz, Spain
E-mail: andres@unex.es and vicenteg@unex.es
URL: http://www.unex.es/eweb/fisteor/andres/ and
http://www.unex.es/eweb/fisteor/vicente/

Received 5 June 2007
Accepted 18 July 2007
Published 10 August 2007

Online at stacks.iop.org/JSTAT/2007/P08021
doi:10.1088/1742-5468/2007/08/P08021

Abstract. The Boltzmann equation for inelastic Maxwell models is considered to determine the velocity moments through the fourth degree in the simple shear flow state. First, the rheological properties (which are related to the second-degree velocity moments) are *exactly* evaluated in terms of the coefficient of restitution α and the (reduced) shear rate a^*. For a given value of α, the above transport properties decrease with increasing shear rate. Moreover, as expected, the third-degree and the asymmetric fourth-degree moments vanish in the long time limit when they are scaled with the thermal speed. On the other hand, our results show that, for a given value of α, the scaled symmetric fourth-degree moments diverge in time for shear rates larger than a certain critical value $a_c^*(\alpha)$ which decreases with increasing dissipation. The explicit shear-rate dependence of the fourth-degree moments below this critical value is also obtained.

Keywords: exact results, granular matter, kinetic theory of gases and liquids, rheology and transport properties

ArXiv ePrint: 0706.0475

J. Stat. Mech. (2007) P08021

Contents

1. Introduction

One of the most widely studied inhomogeneous states in granular gases is the so-called simple or uniform shear flow (USF) [1, 2]. This state is characterized by a constant density n, a uniform granular temperature T, and a linear velocity profile $u_x = ay$, where a is the constant shear rate. The temperature changes over time due to two competing effects: the viscous heating and the inelastic collisional cooling. Depending on the initial condition, one of the effects prevails over the other one so that the temperature either increases or decreases over time, until a steady state is reached for sufficiently long times. After a short kinetic regime, the time evolution and the steady state of the system admits a non-Newtonian hydrodynamic description [3, 4] characterized by shear-rate dependent viscosity and normal stress differences.

The prototypical model of granular gases consists of inelastic hard spheres (IHS) with a constant coefficient of normal restitution $\alpha \leq 1$. In the low density limit, all the relevant information on the system is provided by the one-particle velocity distribution function $f(\mathbf{r}, \mathbf{v}; t)$, which obeys the Boltzmann equation [5]. However, it is generally not possible to get exact analytical results from the Boltzmann equation for IHS, especially in far from equilibrium situations such as the USF. Consequently, most of the analytical results reported in the literature have been derived by using approximations and/or kinetic models [6]–[17].

The lack of exact analytical results can be overcome in some situations by considering the so-called inelastic Maxwell models (IMM), where the collision rate is independent of the relative velocity of the two colliding particles. These models have received a lot of

J. Stat. Mech. (2007) P08021

attention in the last few years since they allow for the derivation of a number of exact results [18]–[44]. Therefore, the influence of inelasticity on the dynamic properties can be analyzed without introducing additional, and sometimes uncontrolled, approximations. In addition, it is interesting to remark that recent experiments [45] for magnetic grains with dipolar interactions turn out to be well described by IMM.

In the context of the USF, the rheological properties, which are related with the second-degree velocity moments, have been obtained exactly in the steady state from the Boltzmann equation for IMM [21, 37]. However, even though these properties are physically important, they provide a partial piece of information about the velocity distribution function f, especially in the high velocity region, where higher degree velocity moments play a prominent role. By symmetry reasons, the third-degree moments are expected to vanish in the USF. Therefore, the first non-trivial moments beyond the ones associated with the rheological properties are the fourth-degree moments. Their knowledge provides relevant information about the combined effect of shearing and inelasticity on the velocity distribution.

The effort of going from second-degree to fourth-degree moments in the USF problem can be justified by a number of reasons. For instance, their knowledge is needed to evaluate transport properties in situations slightly perturbed from the USF state [46], which allows one to perform a linear stability analysis around that state. Another interesting issue is to explore whether or not the divergence of the fourth-degree moments for elastic Maxwell molecules beyond a certain critical shear rate [47]–[49] is also present in the inelastic case and, if so, to what extent.

The main aim of this paper is to determine the fourth-degree moments of IMM subject to USF. This can be carried out thanks to recent derivations by the authors of the fourth-degree collisional moments for IMM [44]. Those moments are proportional to an effective collision frequency ν_0, which in principle can be freely chosen. Here we will consider two classes of IMM: (a) a collision frequency ν_0 independent of temperature (Model A) and (b) a collision frequency $\nu_0(T)$ monotonically increasing with temperature (Model B). While Model A is closer to the original model of Maxwell molecules for elastic gases [47, 50], Model B, with $\nu_0(T) \propto T^{1/2}$, is closer to IHS. The possibility of having a general function $\nu(T)$ is akin to the class of inelastic repulsive models recently introduced by Ernst and co-workers [41, 42]. As will be shown below, Models A and B yield the same results in the steady state. In particular, the reduced shear rate $a^* = a/\nu_0$ in the steady state is a 'universal' well-defined function $a_s^*(\alpha)$ of the coefficient of restitution α. The main feature of Model A is that a^* does not change in time and so a steady state does not exist, except for the specific value $a^* = a_s^*(\alpha)$. However, a non-Newtonian hydrodynamic regime (in which a^* and α are independent and arbitrary parameters) is reached for asymptotically long times. This allows to study analytically the combined effect of both control parameters on the (scaled) velocity moments for Model A.

The plan of the paper is as follows. In section 2, the Boltzmann equation for IMM is introduced and the explicit expressions for the collisional moments through fourth-degree are given. Section 3 deals with the rheological properties (a non-linear shear viscosity η^* and a viscometric function Ψ) of the USF state, which are related to the second-degree velocity moments (pressure tensor). While Model A lends itself to obtain the *exact* forms of η^* and Ψ as non-linear functions of a^* and α, that is not the case for Model B since those rheological quantities require to be solved numerically, except in the

J. Stat. Mech. (2007) P08021

steady state. For elastic collisions ($\alpha = 1$), our expressions of η^* and Ψ obtained for Model A reduce to the results derived long time ago by Ikenberry and Truesdell [51] for Maxwell molecules. The third- and fourth-degree moments for Model A are analyzed in section 4. As expected, the results show that, when the third- and asymmetric fourth-degree moments are conveniently scaled with the thermal speed, they vanish in the long time limit. This is not the case for the symmetric fourth-degree moments. In a way similar to the case of elastic Maxwell molecules [47]–[49], we find that, for a given value of the coefficient of restitution, those moments diverge in time for shear rates larger than a certain critical value $a_c^*(\alpha)$, which decreases as α decreases. Below this critical value, the (scaled) fourth-degree moments have well-defined values in the long time limit. The paper is closed in section 5 with some concluding remarks.

2. The Boltzmann equation for IMM. Collisional moments

In the absence of external forces, the inelastic Boltzmann equation for IMM reads

$$(\partial_t + \mathbf{v}\cdot\nabla) f(\mathbf{r},\mathbf{v};t) = J[\mathbf{v}|f,f], \tag{1}$$

where the Boltzmann collision operator $J[\mathbf{v}|f,f]$ is given by [36]

$$J[\mathbf{v}_1|f,f] = \frac{\nu}{n\Omega_{\rm d}} \int d\mathbf{v}_2 \int d\widehat{\boldsymbol{\sigma}} \left[\alpha^{-1} f(\mathbf{v}_1') f(\mathbf{v}_2') - f(\mathbf{v}_1) f(\mathbf{v}_2)\right]. \tag{2}$$

Here,

$$n = \int d\mathbf{v} f(\mathbf{v}) \tag{3}$$

is the number density, ν is the collision frequency (assumed to be independent of α), $\Omega_{\rm d} = 2\pi^{d/2}/\Gamma(d/2)$ is the total solid angle in d dimensions, and $\alpha \leq 1$ refers to the constant coefficient of restitution. In addition, the primes on the velocities denote the initial values $\{\mathbf{v}_1', \mathbf{v}_2'\}$ that lead to $\{\mathbf{v}_1, \mathbf{v}_2\}$ following a binary collision:

$$\mathbf{v}_1' = \mathbf{v}_1 - \tfrac{1}{2}\left(1+\alpha^{-1}\right)(\widehat{\boldsymbol{\sigma}}\cdot\mathbf{g})\widehat{\boldsymbol{\sigma}}, \qquad \mathbf{v}_2' = \mathbf{v}_2 + \tfrac{1}{2}\left(1+\alpha^{-1}\right)(\widehat{\boldsymbol{\sigma}}\cdot\mathbf{g})\widehat{\boldsymbol{\sigma}}, \tag{4}$$

where $\mathbf{g} = \mathbf{v}_1 - \mathbf{v}_2$ is the relative velocity of the colliding pair and $\widehat{\boldsymbol{\sigma}}$ is a unit vector directed along the centers of the two colliding particles. Apart from n, the basic moments of f are the flow velocity

$$\mathbf{u} = \frac{1}{n}\int d\mathbf{v}\mathbf{v} f(\mathbf{v}) \tag{5}$$

and the granular temperature

$$T = \frac{m}{dn}\int d\mathbf{v}\, V^2 f(\mathbf{v}), \tag{6}$$

where $\mathbf{V} = \mathbf{v} - \mathbf{u}(\mathbf{r})$ is the peculiar velocity. The momentum and energy fluxes are characterized by the pressure tensor

$$P_{ij} = m\int d\mathbf{v}\, V_i V_j f(\mathbf{v}) \tag{7}$$

J. Stat. Mech. (2007) P08021

and the heat flux

$$\mathbf{q} = \frac{m}{2}\int d\mathbf{v}\, V^2 \mathbf{V} f(\mathbf{v}). \tag{8}$$

Finally, the rate of energy dissipated due to collisions defines the cooling rate ζ as

$$\zeta = -\frac{m}{dnT}\int d\mathbf{v}\, V^2 J[\mathbf{v}|f,f]. \tag{9}$$

The main advantage of the Boltzmann equation for Maxwell models (both elastic and inelastic) is that the (collisional) moments of J can be exactly evaluated in terms of the moments of f, without the explicit knowledge of the latter [50]. This property has been recently exploited [44] to obtain the detailed expressions for all the third- and fourth-degree collisional moments as functions of α in d dimensions. In order to get the collisional moments, it is convenient to introduce the Ikenberry polynomials [50] $Y_{2r|i_1 i_2 \ldots i_s}(\mathbf{V})$ of degree $2r+s$. The Ikenberry polynomials of degree smaller than or equal to four are

$$Y_{0|0}(\mathbf{V}) = 1, \qquad Y_{0|i}(\mathbf{V}) = V_i, \tag{10}$$

$$Y_{2|0}(\mathbf{V}) = V^2, \qquad Y_{0|ij}(\mathbf{V}) = V_i V_j - \frac{1}{d}V^2\delta_{ij}, \tag{11}$$

$$Y_{2|i}(\mathbf{V}) = V^2 V_i, \qquad Y_{0|ijk}(\mathbf{V}) = V_i V_j V_k - \frac{1}{d+2}V^2\left(V_i\delta_{jk} + V_j\delta_{ik} + V_k\delta_{ij}\right), \tag{12}$$

$$Y_{4|0}(\mathbf{V}) = V^4, \qquad Y_{2|ij}(\mathbf{V}) = V^2\left(V_i V_j - \frac{1}{d}V^2\delta_{ij}\right), \tag{13}$$

$$\begin{aligned} Y_{0|ijk\ell}(\mathbf{V}) &= V_i V_j V_k V_\ell - \frac{1}{d+4}V^2(V_i V_j\delta_{k\ell} + V_i V_k\delta_{j\ell} + V_i V_\ell\delta_{jk} + V_j V_k\delta_{i\ell} + V_j V_\ell\delta_{ik} \\ &\quad + V_k V_\ell\delta_{ij}) + \frac{1}{(d+2)(d+4)}V^4\left(\delta_{ij}\delta_{k\ell} + \delta_{ik}\delta_{j\ell} + \delta_{i\ell}\delta_{jk}\right) \\ &= V_i V_j V_k V_\ell - \frac{1}{d+4}[Y_{2|ij}(\mathbf{V})\delta_{k\ell} + Y_{2|ik}(\mathbf{V})\delta_{j\ell} + Y_{2|i\ell}(\mathbf{V})\delta_{jk} + Y_{2|jk}(\mathbf{V})\delta_{i\ell} \\ &\quad + Y_{2|j\ell}(\mathbf{V})\delta_{ik} + Y_{2|k\ell}(\mathbf{V})\delta_{ij}] - \frac{1}{d(d+2)}V^4(\delta_{ij}\delta_{k\ell} + \delta_{ik}\delta_{j\ell} + \delta_{i\ell}\delta_{jk}). \end{aligned} \tag{14}$$

The corresponding velocity moments $M_{2r|i_1 i_2 \ldots i_s}$ and collisional moments $J_{2r|i_1 i_2 \ldots i_s}$ are defined, respectively, as

$$M_{2r|i_1 i_2 \ldots i_s} = \int d\mathbf{v}\, Y_{2r|i_1 i_2 \ldots i_s}(\mathbf{V}) f(\mathbf{v}), \tag{15}$$

$$J_{2r|i_1 i_2 \ldots i_s} = \int d\mathbf{v}\, Y_{2r|i_1 i_2 \ldots i_s}(\mathbf{V}) J[\mathbf{v}|f,f]. \tag{16}$$

In particular, $M_{0|0} = n$, $M_{0|i} = 0$ (by definition of the peculiar velocity), $M_{2|0} = pd/m$, where $p = nT$ is the hydrostatic pressure, $M_{0|ij} = (P_{ij} - p\delta_{ij})/m$, and $M_{2|i} = 2q_i/m$. Moreover, conservation of mass and momentum implies $J_{0|0} = 0$ and $J_{0|i} = 0$, respectively, while $J_{2|0} = -\zeta M_{2|0}$.

J. Stat. Mech. (2007) P08021

The explicit expressions for the collisional moments $J_{2r|i_1i_2\ldots i_s}$ for $2r+s\leq 4$ are [44]

$$J_{2|0}=-\zeta M_{2|0},\qquad J_{0|ij}=-\nu_{0|2}M_{0|ij}, \tag{17}$$

$$J_{2|i}=-\nu_{2|1}M_{2|i},\qquad J_{0|ijk}=-\nu_{0|3}M_{0|ijk}, \tag{18}$$

$$J_{4|0}=-\nu_{4|0}M_{4|0}+\lambda_1 n^{-1}M_{2|0}^2-\lambda_2 n^{-1}M_{0|ij}M_{0|ji}, \tag{19}$$

$$J_{2|ij}=-\nu_{2|2}M_{2|ij}+\lambda_3 n^{-1}M_{2|0}M_{0|ij}-\lambda_4 n^{-1}\left(M_{0|ik}M_{0|kj}-\frac{1}{d}M_{0|k\ell}M_{0|\ell k}\delta_{ij}\right), \tag{20}$$

$$\begin{aligned}J_{0|ijk\ell}=&-\nu_{0|4}M_{0|ijk\ell}+\lambda_5 n^{-1}\Big[M_{0|ij}M_{0|k\ell}+M_{0|ik}M_{0|j\ell}+M_{0|i\ell}M_{0|jk}-\frac{2}{d+4}\\&\times\left(M_{0|ip}M_{0|pj}\delta_{k\ell}+M_{0|ip}M_{0|pk}\delta_{j\ell}+M_{0|ip}M_{0|p\ell}\delta_{jk}+M_{0|jp}M_{0|pk}\delta_{i\ell}\right.\\&\left.+M_{0|jp}M_{0|p\ell}\delta_{ik}+M_{0|kp}M_{0|p\ell}\delta_{ij}\right)+\frac{2}{(d+2)(d+4)}M_{0|pq}M_{0|qp}\\&\times\left(\delta_{ij}\delta_{k\ell}+\delta_{ik}\delta_{j\ell}+\delta_{i\ell}\delta_{jk}\right)\Big].\end{aligned} \tag{21}$$

In equations (19)–(21), the usual summation convention over repeated indices is assumed. The cooling rate ζ and the effective collision frequencies $\nu_{2r|s}$ are given by the expressions

$$\zeta=\frac{d+2}{4d}\left(1-\alpha^2\right)\nu_0, \tag{22}$$

$$\nu_{0|2}=\zeta+\frac{(1+\alpha)^2}{4}\nu_0, \tag{23}$$

$$\nu_{2|1}=\tfrac{3}{2}\zeta+\frac{(1+\alpha)^2(d-1)}{4d}\nu_0, \tag{24}$$

$$\nu_{0|3}=\tfrac{3}{2}\nu_{0|2}, \tag{25}$$

$$\nu_{4|0}=2\zeta+\frac{(1+\alpha)^2\left(4d-7+6\alpha-3\alpha^2\right)}{16d}\nu_0, \tag{26}$$

$$\nu_{2|2}=2\zeta+\frac{(1+\alpha)^2\left[3d^2+7d-14+3\alpha(d+4)-6\alpha^2\right]}{8d(d+4)}\nu_0, \tag{27}$$

$$\nu_{0|4}=2\zeta+\frac{(1+\alpha)^2\left[d^3+9d^2+17d-9+3\alpha(d+4)-3\alpha^2\right]}{2d(d+4)(d+6)}\nu_0, \tag{28}$$

where we have called $\nu_0\equiv 2\nu/(d+2)$. According to equations (17) and (23), ν_0 represents the effective collision frequency associated with the shear viscosity in the elastic limit [52]. Finally, the cross coefficients λ_i in equations (19)–(21) are

$$\lambda_1=\frac{(1+\alpha)^2(d+2)\left(4d-1-6\alpha+3\alpha^2\right)}{16d^2}\nu_0, \tag{29}$$

$$\lambda_2 = \frac{(1+\alpha)^2\,(1+6\alpha-3\alpha^2)}{8d}\nu_0, \tag{30}$$

$$\lambda_3 = \frac{(1+\alpha)^2\,[d^2+5d-2-3\alpha(d+4)+6\alpha^2]}{8d^2}\nu_0, \tag{31}$$

$$\lambda_4 = \frac{(1+\alpha)^2\,[2-d+3\alpha(d+4)-6\alpha^2]}{4d(d+4)}\nu_0, \tag{32}$$

$$\lambda_5 = \frac{(1+\alpha)^2\,[d^2+7d+9-3\alpha(d+4)+3\alpha^2]}{2d(d+4)(d+6)}\nu_0. \tag{33}$$

The above results hold independently of the specific form of the collision frequency ν_0. On physical grounds, $\nu_0 \propto n$. In the case of *elastic* Maxwell molecules, ν_0 is independent of temperature. The extension of this feature to the inelastic case defines Model A. On the other hand, one can assume that ν_0 is an increasing function of temperature (Model B). In particular $\nu_0(T) \propto nT^{1/2}$ makes Model B mimic the properties of IHS.

3. Uniform shear flow. Rheological properties

3.1. Hierarchy of moment equations

Let us assume that the gas is under the USF. As said in the Introduction, this state is macroscopically defined by a constant density n, a spatially uniform temperature $T(t)$, and a linear flow velocity $\mathbf{u}(y) = ay\widehat{\mathbf{x}}$ [47]. At a microscopic level, the USF is characterized by a velocity distribution function that becomes *uniform* in the local Lagrangian frame, i.e.,

$$f(\mathbf{r},\mathbf{v};t) = f(\mathbf{V},t). \tag{34}$$

In this frame, the Boltzmann equation (1) reduces to

$$\partial_t f(\mathbf{V}) - aV_y\frac{\partial}{\partial V_x}f(\mathbf{V}) = J[\mathbf{V}|f,f]. \tag{35}$$

Equation (35) is invariant under the transformations

$$(V_x,V_y) \to (-V_x,-V_y), \tag{36}$$

$$V_j \to -V_j, \qquad j \neq x,y. \tag{37}$$

This implies that if the initial state $f(\mathbf{V},0)$ is consistent with the symmetry properties (36) and (37) so is the solution to equation (35) at any time $t > 0$. Even if one starts from an initial condition inconsistent with (36) and (37), it is expected that the solution asymptotically tends for long times to a function compatible with (36) and (37). The investigation of this expectation, at the level of moments of degree less than or equal to four, is one of the objectives of this paper.

The properties of uniform temperature and constant density and shear rate are enforced in computer simulations by applying the Lees–Edwards boundary conditions [47, 53], regardless of the particular interaction model considered. In the case

J. Stat. Mech. (2007) P08021

of boundary conditions representing realistic plates in relative motion, the corresponding non-equilibrium state is the so-called Couette flow, where density, temperature, and shear rate are no longer uniform [54].

Multiplying both sides of equation (35) by $Y_{r|i_1i_2\ldots i_s}(\mathbf{V})$ and integrating over $\mathbf{V}$ one gets

$$\partial_t M_{r|i_1i_2\ldots i_s} + aN_{r|i_1i_2\ldots i_s} = J_{r|i_1i_2\ldots i_s}, \tag{38}$$

where we have called

$$N_{r|i_1i_2\ldots i_s} \equiv \int \mathrm{d}\mathbf{V}\, f(\mathbf{V}) V_y \frac{\partial}{\partial V_x} Y_{r|i_1i_2\ldots i_s}(\mathbf{V}). \tag{39}$$

In particular,

$$N_{2|0} = 2M_{0|xy}, \qquad N_{0|yy} = -\frac{2}{d}M_{0|xy}, \qquad N_{0|xy} = M_{0|yy} + \frac{1}{d}M_{2|0}, \tag{40}$$

$$N_{0|ij} = M_{0|iy}\delta_{jx} + M_{0|jy}\delta_{ix} + \frac{1}{d}M_{2|0}(\delta_{ix}\delta_{jy} + \delta_{jx}\delta_{iy}) - \frac{2}{d}M_{0|xy}\delta_{ij}, \tag{41}$$

$$N_{4|0} = 4M_{2|xy}. \tag{42}$$

More in general, since $V_y\partial_{V_x}Y_{r|i_1i_2\ldots i_s}(\mathbf{V})$ is a polynomial of degree $2r+s$, the quantity $N_{r|i_1i_2\ldots i_s}$ can be expressed as a linear combination of moments of the same degree. In addition, thanks to the structure of the collision operator for IMM, the collisional moments $J_{r|i_1i_2\ldots i_s}$ only involve moments of degree equal to or smaller than $2r+s$. Consequently, the hierarchy (38) can be exactly solved in a recursive way. We will call *asymmetric* moments those that vanish for velocity distributions compatible with the invariance properties (36) and (37). The remaining moments will be referred to as *symmetric* moments. In particular, all the moments of odd degree are asymmetric. Among the moments of even degree, $M_{2r|xz}$ and $M_{2r|xxxy}$, for instance, are also asymmetric.

In the particular case of the moment $M_{2|0} = nTd/m$, equation (38) becomes

$$\partial_t M_{2|0} + 2aM_{0|xy} = -\zeta M_{2|0}, \tag{43}$$

where use has been made of equation (17). This is not but the balance equation for the energy in the USF. It is convenient to introduce the *scaled* moments

$$M^*_{2r|i_1i_2\ldots i_s} = \frac{1}{nv_0^{2r+s}} M_{2r|i_1i_2\ldots i_s}, \qquad v_0 \equiv \sqrt{\frac{2T}{m}} = \sqrt{\frac{2M_{2|0}}{dn}}, \tag{44}$$

v_0 being the thermal speed, and the reduced shear rate

$$a^* \equiv \frac{a}{\nu_0}. \tag{45}$$

In terms of these scaled variables, equation (38) can be rewritten as

$$\frac{1}{\nu_0}\partial_t M^*_{r|i_1i_2\ldots i_s} + a^* N^*_{r|i_1i_2\ldots i_s} - \left(r + \frac{s}{2}\right)\left(\zeta^* + \frac{4}{d}a^* M^*_{0|xy}\right) M^*_{r|i_1i_2\ldots i_s} = J^*_{r|i_1i_2\ldots i_s}, \tag{46}$$

where $\zeta^* \equiv \zeta/\nu_0$ and

$$N^*_{r|i_1i_2\ldots i_s} \equiv \frac{1}{nv_0^{2r+s}} N_{r|i_1i_2\ldots i_s}, \qquad J^*_{r|i_1i_2\ldots i_s} \equiv \frac{1}{\nu_0 nv_0^{2r+s}} J_{r|i_1i_2\ldots i_s}. \tag{47}$$

It is apparent that the evolution equation (46) involves the second-degree moment $M^*_{0|xy} = P_{xy}/2p$, which is the (reduced) shear stress. This quantity, along with the normal stress differences $M^*_{0|xx} = (P_{xx} - p)/2p$ and $M^*_{0|yy} = (P_{yy} - p)/2p$, are the most relevant ones from a rheological point of view. They will be analyzed in the next subsection.

J. Stat. Mech. (2007) P08021

3.2. Second-degree moments

From equation (46) one gets a coupled set of equations for the moments $M^*_{0|xy}$ and $M^*_{0|yy}$:

$$\frac{1}{\nu_0}\partial_t M^*_{0|xy} + a^*\left(M^*_{0|yy}+\frac{1}{2}\right) + \left(\omega_{0|2} - \frac{4}{d}a^* M^*_{0|xy}\right) M^*_{0|xy} = 0, \tag{48}$$

$$\frac{1}{\nu_0}\partial_t M^*_{0|yy} - \frac{2}{d}a^* M^*_{0|xy} + \left(\omega_{0|2} - \frac{4}{d}a^* M^*_{0|xy}\right) M^*_{0|yy} = 0, \tag{49}$$

where we have introduced the (reduced) shifted quantities

$$\omega_{2r|s} \equiv \frac{\nu_{2r|s} - (r+s/2)\zeta}{\nu_0}, \tag{50}$$

so that

$$\omega_{0|2} = \frac{(1+\alpha)^2}{4}. \tag{51}$$

To close the set, we need in general the evolution equation for the reduced shear rate a^*. From equation (43) is straightforward to obtain

$$\frac{1}{\nu_0}\partial_t a^* = a^*\left(\zeta^* + \frac{4}{d}a^* M^*_{0|xy}\right)\frac{\partial \ln \nu_0}{\partial \ln T}. \tag{52}$$

3.2.1. Model A. Hydrodynamic solution. In Model A the collision frequency ν_0 is independent of temperature and thus it is a constant. Consequently, $\partial_t a^* = 0$ so that the reduced shear rate a^* remains in its initial value (regardless of the value of the coefficient of restitution α) and represents a control parameter measuring the departure of the system from the homogeneous cooling state.

As in the elastic case [47, 50], it is easy to check that, after a certain kinetic regime lasting a few collision times, the scaled moments $M^*_{0|xy}$ and $M^*_{0|yy}$ reach well-defined stationary values, which are non-linear functions of α and $a^* \equiv a/\nu_0$. From equations (48) and (49), one has

$$-M^*_{0|xy}\left(1 - \frac{4}{d}\widetilde{a}M^*_{0|xy}\right) = \widetilde{a}\left(M^*_{0|yy}+\frac{1}{2}\right), \tag{53}$$

$$M^*_{0|yy}\left(1 - \frac{4}{d}\widetilde{a}M^*_{0|xy}\right) = \frac{2}{d}\widetilde{a}M^*_{0|xy} \tag{54}$$

for the stationary values, where we have defined

$$\widetilde{a} \equiv \frac{a^*}{\omega_{0|2}} = \frac{4a^*}{(1+\alpha)^2}. \tag{55}$$

The solution to the set of equations (53) and (54) is

$$M^*_{0|yy} = -\frac{\gamma(\widetilde{a})}{1+2\gamma(\widetilde{a})}, \qquad M^*_{0|xy} = -\frac{d}{2}\frac{\gamma(\widetilde{a})}{\widetilde{a}} = -\frac{\widetilde{a}/2}{[1+2\gamma(\widetilde{a})]^2}, \tag{56}$$

where

$$\gamma(\widetilde{a}) = \frac{2}{3}\sinh^2\left[\frac{1}{6}\cosh^{-1}\left(1+\frac{27}{d}\widetilde{a}^2\right)\right] \tag{57}$$

J. Stat. Mech. (2007) P08021

is the real root of the cubic equation

$$\gamma(1+2\gamma)^2=\frac{\widetilde{a}^2}{d}. \tag{58}$$

Note that the reduced second-degree moments depend on α and a^* through the scaled quantity $\widetilde{a}$ only. From equation (46) it is also easy to prove that, for long times, the normal stresses $M^*_{zz},\ldots,M^*_{dd}$ along directions orthogonal to the shear plane xy are equal to M^*_{yy}. Consequently, $M^*_{0|xx}=-(d-1)M^*_{0|yy}$. Analogously, the asymmetric second-degree moments (i.e., all the off-diagonal elements $M^*_{0|ij}$ except $M^*_{0|xy}$) vanish.

It is convenient to define a non-linear shear viscosity η^* and a viscometric function Ψ as

$$\eta^*(a^*)=-\frac{\nu_0}{p}\frac{P_{xy}}{a}=-2\frac{M^*_{0|xy}}{a^*}, \tag{59}$$

$$\Psi(a^*)=\frac{\nu_0^2}{p}\frac{P_{xx}-P_{yy}}{a^2}=2\frac{M^*_{0|xx}-M^*_{0|yy}}{a^{*2}}. \tag{60}$$

From equations (56) and (58), we have

$$\eta^*(a^*)=\left(\frac{2}{1+\alpha}\right)^2\frac{1}{\left[1+2\gamma(\widetilde{a})\right]^2}, \tag{61}$$

$$\Psi(a^*)=\left(\frac{2}{1+\alpha}\right)^4\frac{2}{\left[1+2\gamma(\widetilde{a})\right]^3}. \tag{62}$$

Interestingly enough, the combination

$$\frac{[\eta^*(a^*)]^3}{[\Psi(a^*)]^2}=\left(\frac{1+\alpha}{4}\right)^2 \tag{63}$$

is independent of the shear rate. Moreover, in the limit of small shear rate (for fixed α), equation (58) implies that $\gamma\to 0$, so that equations (61) and (62) reduce to

$$\eta^*(0)=\frac{4}{(1+\alpha)^2},\qquad \Psi(0)=\frac{32}{(1+\alpha)^4}. \tag{64}$$

The quantities $\eta^*(0)$ and $\Psi(0)$ are the NS shear viscosity and the Burnett value of the viscometric function, respectively, of Model A.

It is important to remark that, although the scaled moments reach stationary values, the system is not in general in a steady state since the temperature changes in time. Actually, inserting the second expression of (56) into equation (43), we get

$$\frac{1}{\nu_0}\partial_t\ln T=-2\omega_{0|2}\left[\gamma_s-\gamma(\widetilde{a})\right], \tag{65}$$

where we have called

$$\gamma_s\equiv\frac{\zeta^*}{2\omega_{0|2}}=\frac{d+2}{2d}\frac{1-\alpha}{1+\alpha}. \tag{66}$$

Equation (65) shows that $T(t)$ either grows or decays exponentially. The first situation occurs if $\gamma(\widetilde{a})>\gamma_s$. In that case, the imposed shear rate is sufficiently large (or the

J. Stat. Mech. (2007) P08021

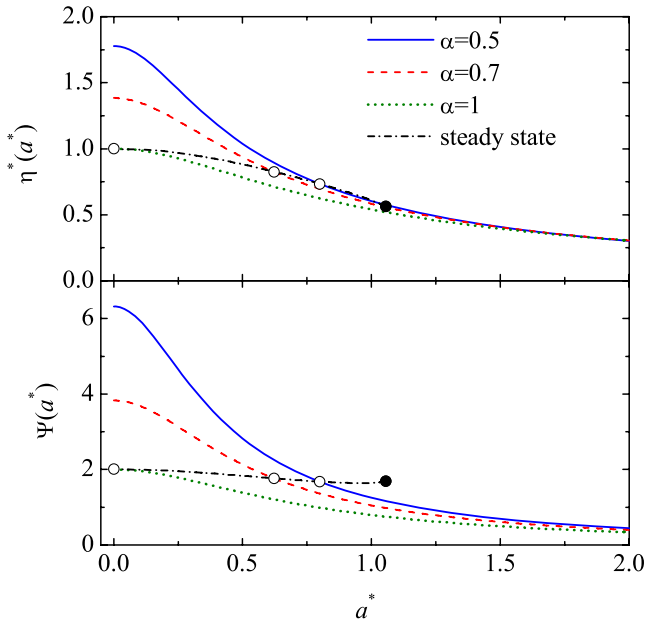

Figure 1. Plot of $\eta^*(a^*)$ (top panel) and $\Psi(a^*)$ (bottom panel) as functions of a^* for $d = 3$ and $\alpha = 0.5$ (solid lines), $\alpha = 0.7$ (dashed lines), and $\alpha = 1$ (dotted lines). The dash–dotted lines are the loci of steady-state points (a_s^*, η_s^*) and (a_s^*, Ψ_s). They intercept the curves representing $\eta^*(a^*)$ and $\Psi(a^*)$ at the steady-state values indicated by circles. Note that the loci end at the points $(a_s^*, \eta_s^*) = (1.054, 0.563)$ and $(a_s^*, \Psi_s) = (1.054, 1.688)$ corresponding to $\alpha = 0$ (represented by filled circles).

inelasticity is sufficiently low) as to make the viscous heating effect dominate over the inelastic cooling effect. The opposite happens if $\gamma(\widetilde{a}) < \gamma_s$. A perfect balance between both effects takes place if $\gamma(\widetilde{a}) = \gamma_s$. Inserting this condition into equation (58) one gets the steady-state point

$$a_s^* = \omega_{0|2}\sqrt{d\gamma_s}(1+2\gamma_s) = \sqrt{\frac{d+2}{2}(1-\alpha^2)}\frac{d+1-\alpha}{2d}. \tag{67}$$

In this state, the α-dependence of the rheological properties is

$$\eta_s^* = \eta^*(a_s^*) = \left(\frac{d}{d+1-\alpha}\right)^2, \qquad \Psi_s = \Psi(a_s^*) = \frac{4}{1+\alpha}\left(\frac{d}{d+1-\alpha}\right)^3. \tag{68}$$

Equations (67) and (68) agree with the results reported in [37], while the more general expressions (61) and (62) had not been previously derived.

Figure 1 shows the shear-rate dependence of the rheological functions $\eta^*(a^*)$ and $\Psi(a^*)$ for $d = 3$ and three values of the coefficient of restitution: $\alpha = 0.5$ (highly inelastic system), $\alpha = 0.7$ (moderately inelastic system), and $\alpha = 1$ (elastic system). The steady-state points (a_s^*, η_s^*) and (a_s^*, Ψ_s) are also represented by circles for each one of the values of α. Given a value of α, the steady-state point splits each curve into two branches: the one with $a^* > a_s^*$ corresponds to $\gamma(\widetilde{a}) > \gamma_s$ and so the temperature increases in time, while the branch with $a^* < a_s^*$ corresponds to states with a decreasing temperature. We observe

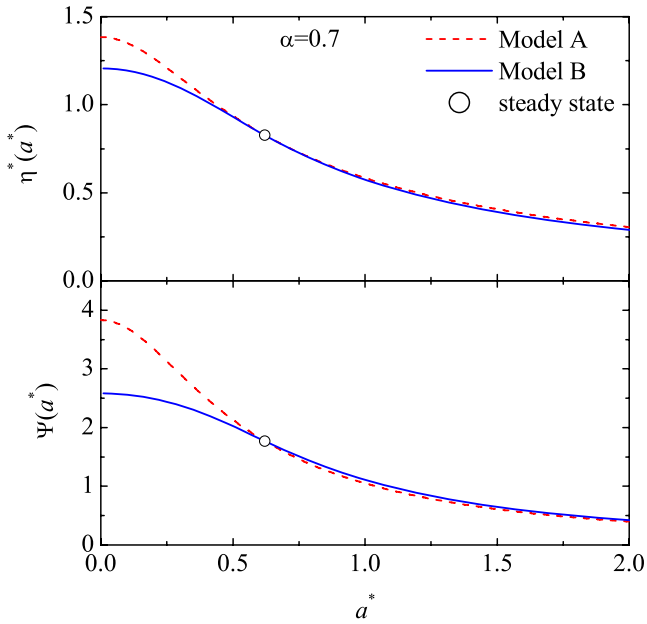

Figure 2. Plot of $\eta^*(a^*)$ (top panel) and $\Psi(a^*)$ (bottom panel) as functions of a^* for $d = 3$ and $\alpha = 0.7$. The dashed and solid lines correspond to Model A (equations (61) and (62)) and Model B with $\nu_0(T) \propto T^{1/2}$ (numerical solution of equations (48)–(52)), respectively. The circles represent the steady-state points (a_s^*, η_s^*) and (a_s^*, Ψ_s), which are common to Models A and B.

that, for a given value of α, both $\eta^*(a^*)$ and $\Psi(a^*)$ decrease with increasing shear rate. In the region of high shear rates (say $a^* > 1.5$), the curves are practically insensitive to the value of the coefficient of restitution. For small and moderate shear rates, however, the influence of α is noticeable: at a given value of the reduced shear rate a^*, the rheological quantities $\eta^*(a^*)$ and $\Psi(a^*)$ increase as α decreases. On the other hand, the steady-state values η_s^* and Ψ_s^* decrease with increasing dissipation.

3.2.2. Model B. Steady-state solution. In Model B the collision frequency $\nu_0(T)$ is an increasing function of temperature, and so the reduced shear rate a^* is not constant. The corresponding steady-state solution is obtained from equations (43)–(52) by setting $\partial_t \to 0$. It is given again by equations (56)–(58), except that now $\gamma(\widetilde{a}) \to \gamma_s$ and $\widetilde{a} \to a_s^*/\omega_{0|2}$, where γ_s and a_s^* are given by equations (66) and (67), respectively. Therefore, the steady-state results are "universal" in the sense that they hold both for Model A and Model B, regardless of the precise dependence $\nu_0(T)$.

In order to have $M_{0|xy}^*(a^*)$ and $M_{0|yy}^*(a^*)$ in Model B, one has to solve numerically the non-linear coupled set (48)–(52), discard the kinetic stage of the evolution, and eliminate time in favor of a^* [3]. The resulting rheological curves are illustrated in figure 2 at $\alpha = 0.7$ and for the choice $\nu_0(t) \propto T^{1/2}$ in Model B. Comparison with the analytical results corresponding to Model A shows that the influence of the temperature dependence of ν_0 on the rheological properties is only significant for reduced shear rates smaller than the steady-state one. Since in this paper we want to focus on analytical results, henceforth we will only consider Model A, except for what concerns the common steady state of Models A and B.

J. Stat. Mech. (2007) P08021

4. Third- and fourth-degree moments

In this section we will analyze, in the context of Model A, the time evolution and the stationary values of the (scaled) third- and fourth-degree moments in the USF problem. The results will depend on both the reduced shear rate a^* and the coefficient of restitution α, while they only depend on the latter in the common steady state.

Let us assume that the scaled second-degree moments have reached their stationary values given by equation (56). Therefore, equation (46) becomes

$$\partial_s M^*_{r|i_1i_2\ldots i_s} + a^* N^*_{r|i_1i_2\ldots i_s} - \left(r+\frac{s}{2}\right)\left[\zeta^* - 2\omega_{0|2}\gamma(\widetilde{a})\right] M^*_{r|i_1i_2\ldots i_s} = J^*_{r|i_1i_2\ldots i_s}, \tag{69}$$

where $\mathrm{d}s = \nu_0\,\mathrm{d}t$. In what follows we will particularize to a three-dimensional gas ($d=3$).

4.1. Third-degree moments

As said in the preceding section, all the third-degree moments are asymmetric and so they are expected to vanish for long times. Here we want to confirm this expectation and get the corresponding relaxation rates.

In a three-dimensional system, there are 10 independent third-degree moments. Here we take

$$\{M^*_{2|x}, M^*_{2|y}, M^*_{2|z}, M^*_{0|xxy}, M^*_{0|xxz}, M^*_{0|xyy}, M^*_{0|yyz}, M^*_{0|xzz}, M^*_{0|yzz}, M^*_{0|xyz}\}. \tag{70}$$

From equation (69) and making use of the third-degree collisional moments (cf equation (18)) and of the definition (39), one gets the following set of equations:

$$\left[\partial_s + \omega_{0|3} + 3\omega_{0|2}\gamma(\widetilde{a})\right]\left(\tfrac{1}{4}M^*_{0|xxz} + M^*_{0|yyz}\right) = 0, \tag{71}$$

$$\left[\partial_s + \omega_{0|3} + 3\omega_{0|2}\gamma(\widetilde{a})\right]\left(\tfrac{1}{4}M^*_{0|xxy} + M^*_{0|yzz}\right) = 0, \tag{72}$$

$$\begin{pmatrix} \partial_s + \omega_{2|1} + 3\omega_{0|2}\gamma(\widetilde{a}) & 0 & 2a^* \\ 0 & \partial_s + \omega_{0|3} + 3\omega_{0|2}\gamma(\widetilde{a}) & -\frac{2}{5}a^* \\ \frac{1}{5}a^* & a^* & \partial_s + \omega_{0|3} + 3\omega_{0|2}\gamma(\widetilde{a}) \end{pmatrix} \times \begin{pmatrix} M^*_{2|z} \\ M^*_{0|yyz} \\ M^*_{0|xyz} \end{pmatrix} = \begin{pmatrix} 0 \\ 0 \\ 0 \end{pmatrix}, \tag{73}$$

$$\begin{pmatrix} \partial_s + \omega_{2|1} + 3\omega_{0|2}\gamma(\widetilde{a}) & \frac{7}{5}a^* & 2a^* & 0 \\ \frac{2}{5}a^* & \partial_s + \omega_{2|1} + 3\omega_{0|2}\gamma(\widetilde{a}) & 0 & 2a^* \\ \frac{8}{25}a^* & 0 & \partial_s + \omega_{0|3} + 3\omega_{0|2}\gamma(\widetilde{a}) & \frac{8}{5}a^* \\ 0 & \frac{8}{25}a^* & -\frac{23}{20}a^* & \partial_s + \omega_{0|3} + 3\omega_{0|2}\gamma(\widetilde{a}) \end{pmatrix} \times \begin{pmatrix} M^*_{2|x} \\ M^*_{2|y} \\ M^*_{0|xxy} \\ M^*_{0|xyy} \end{pmatrix} = a^*\left(\tfrac{1}{4}M^*_{0|xxy} + M^*_{0|yzz}\right)\begin{pmatrix} 0 \\ 0 \\ 0 \\ 1 \end{pmatrix}, \tag{74}$$

$$\left[\partial_s + \omega_{0|3} + 3\omega_{0|2}\gamma(\widetilde{a})\right] M^*_{0|xzz} = a^*\left(\tfrac{2}{5}M^*_{2|y} + \tfrac{2}{5}M^*_{0|xxy} - M^*_{0|yzz}\right). \tag{75}$$

J. Stat. Mech. (2007) P08021

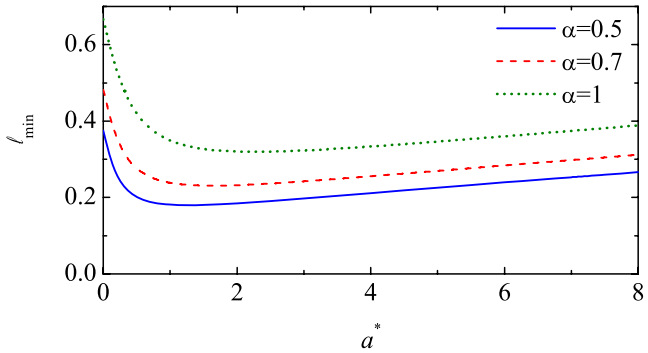

Figure 3. Plot of the smallest eigenvalue, $\ell_{\min}$, associated with the time evolution of the third-degree moments as a function of a^* for $d = 3$ and $\alpha = 0.5$ (solid line), $\alpha = 0.7$ (dashed line), and $\alpha = 1$ (dotted line).

The characteristic equations associated with equations (71)–(75) are

$$\ell = \omega_{0|3} + 3\omega_{0|2}\gamma(\widetilde{a}) = \tfrac{3}{4}(1+\alpha)^2\left[\gamma(\widetilde{a}) + \tfrac{1}{2}\right], \tag{76}$$

$$\left[\omega_{0|3} + 3\omega_{0|2}\gamma(\widetilde{a}) - \ell\right]^2\left[\omega_{2|1} + 3\omega_{0|2}\gamma(\widetilde{a}) - \ell\right] = \frac{2(\omega_{0|3} - \omega_{2|1})}{5}a^{*2}, \tag{77}$$

$$\begin{aligned}\left[\omega_{0|3} + 3\omega_{0|2}\gamma(\widetilde{a}) - \ell\right]^2&\left[\omega_{2|1} + 3\omega_{0|2}\gamma(\widetilde{a}) - \ell\right]^2 \\ &= \frac{2(\omega_{0|3} - \omega_{2|1})}{25}a^{*2}\left[7\omega_{0|3} + 23\omega_{2|1} + 30\left(3\omega_{0|2}\gamma(\widetilde{a}) - \ell\right)\right],\end{aligned} \tag{78}$$

where ℓ denotes the corresponding eigenvalues. The time evolution for long times is governed by the eigenvalue $\ell_{\min}$ with the smallest real part. It can be checked that $\ell_{\min}$ (which is the smallest real root of the quartic equation (78)) is positive definite for all α and a^*. Consequently, all the scaled third-degree moments vanish in the long time limit, as expected by symmetry arguments. In addition, at a given value of a^*, the larger the inelasticity the longer the relaxation time (which is proportional to $\ell_{\min}^{-1}$). The shear-rate dependence of $\ell_{\min}$ is plotted in figure 3 for the same values of α as considered before. It is interesting to remark that $\ell_{\min}$ is not a monotonic function of a^*, reaching a minimum value at a certain shear rate.

4.2. Fourth-degree moments

In a three-dimensional system, there are 15 independent fourth-degree moments, of which 9 are symmetric and 6 are symmetric, in the sense described at the beginning of section 3.

4.2.1. Asymmetric moments. Because of the symmetries of equation (35), the symmetric and asymmetric moments are uncoupled. Although the relevant moments are the symmetric ones, we first analyze the time evolution of the asymmetric moments, for the sake of completeness. As the set of asymmetric moments, we choose

$$\{M^*_{2|xz}, M^*_{2|yx}, M^*_{0|xxxzy}, M^*_{0|yyyz}, M^*_{0|xzzz}, M^*_{0|yzzz}\}. \tag{79}$$

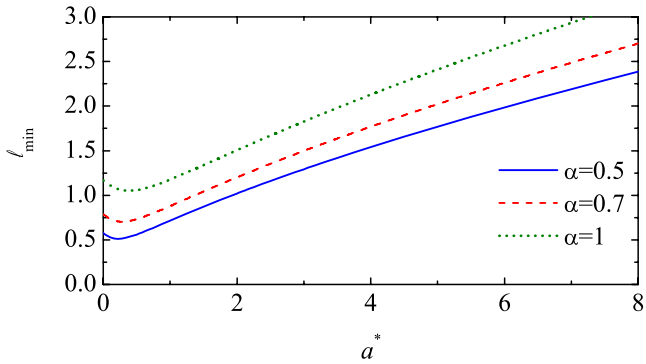

Figure 4. Plot of the smallest eigenvalue, $\ell_{\min}$, associated with the time evolution of the asymmetric fourth-degree moments as a function of a^* for $d = 3$ and $\alpha = 0.5$ (solid line), $\alpha = 0.7$ (dashed line), and $\alpha = 1$ (dotted line).

They verify the following set of equations:

$$\left[\partial_s + \omega_{0|4} + 4\omega_{0|2}\gamma(\widetilde{a})\right]\left(M^*_{0|yyyz} - M^*_{0|yzzz}\right) = 0, \tag{80}$$

$$\begin{pmatrix} \partial_s + \omega_{2|2} + 4\omega_{0|2}\gamma(\widetilde{a}) & \frac{9}{7}a^* & 0 & -2a^* \\ \frac{2}{7}a^* & \partial_s + \omega_{2|2} + 4\omega_{0|2}\gamma(\widetilde{a}) & -2a^* & 0 \\ 0 & -\frac{12}{49}a^* & \partial_s + \omega_{0|4} + 4\omega_{0|2}\gamma(\widetilde{a}) & -\frac{11}{14}a^* \\ -\frac{12}{49}a^* & 0 & \frac{12}{7}a^* & \partial_s + \omega_{0|4} + 4\omega_{0|2}\gamma(\widetilde{a}) \end{pmatrix} \times \begin{pmatrix} M^*_{2|xz} \\ M^*_{2|yz} \\ M^*_{0|xxxz} + M^*_{0|xzzz} \\ M^*_{0|yyyz} + M^*_{0|yzzz} \end{pmatrix} = \frac{1}{2}a^*(M^*_{0|yyyz} - M^*_{0|yzzz}) \begin{pmatrix} 0 \\ 0 \\ 1 \\ 0 \end{pmatrix}, \tag{81}$$

$$\left[\partial_s + \omega_{0|4} + 4\omega_{0|2}\gamma(\widetilde{a})\right]\left(M^*_{0|xxxz} - M^*_{0|xzzz}\right) = \tfrac{7}{2}a^*(M^*_{0|yyyz} + M^*_{0|yzzz}) - \tfrac{1}{2}a^*(M^*_{0|yyyz} - M^*_{0|yzzz}). \tag{82}$$

The eigenvalues associated with the time behavior of the asymmetric fourth-degree moments are

$$\ell = \omega_{0|4} + 4\omega_{0|2}\gamma(\widetilde{a}) = (1+\alpha)^2\left[\gamma(\widetilde{a}) + \frac{50 + 7\alpha - \alpha^2}{126}\right] \tag{83}$$

and the roots of the characteristic quartic equation

$$\left[\omega_{0|4} + 4\omega_{0|2}\gamma(\widetilde{a}) - \ell\right]^2\left[\omega_{2|2} + 4\omega_{0|2}\gamma(\widetilde{a}) - \ell\right]^2 = \frac{6(\omega_{0|4} - \omega_{2|2})}{49}a^{*2}\left[3\omega_{0|4} + 11\omega_{2|2} + 14\left(4\omega_{0|4}\gamma(\widetilde{a}) - \ell\right)\right]. \tag{84}$$

All the eigenvalues have a positive real part. Therefore, all the asymmetric moments defined in equation (79) decay to zero in the long time limit, the final stage being characterized by the smallest real root $\ell_{\min}$ of equation (84). This eigenvalue is plotted in figure 4 for the same cases as in figure 3. Again, a non-monotonic behavior is observed. On the other hand, for given values of a^* and α, the value of $\ell_{\min}$ corresponding to the third-degree moments is smaller than the one corresponding to the asymmetric fourth-degree moments.

4.2.2. Symmetric moments. In parallel to the elastic case [47], we choose the following set of 9 symmetric moments

$$\{M^*_{4|0}, M^*_{2|xx}, M^*_{2|yy}, M^*_{2|xy}, M^*_{0|xxxx}, M^*_{0|yyyy}, M^*_{0|zzzz}, M^*_{0|xxxy}, M^*_{0|xyyy}\}. \tag{85}$$

The combination

$$\mathcal{M}_9 \equiv 3M^*_{0|xxxx} - 4M^*_{0|yyyy} - 4M^*_{0|zzzz} = \frac{1}{nv_0^4}\int \mathrm{d}\mathbf{V}\left(6V_y^2V_z^2 - V_y^4 - V_z^4\right) f(\mathbf{V}) \tag{86}$$

is the average of a quantity independent of V_x, so the associated combination $3N^*_{0|xxxx} - 4N^*_{0|yyyy} - 4N^*_{0|zzzz}$ vanishes. Moreover, the combination $3J^*_{0|xxxx} - 4J^*_{0|yyyy} - 4J^*_{0|zzzz} = -\nu_{0|4}\mathcal{M}_9$ due to the fact that $M_{0|yy} = M_{0|zz}$. Therefore, equation (69) yields

$$\left[\partial_s + \omega_{0|4} + 4\omega_{0|2}\gamma(\widetilde{a})\right]\mathcal{M}_9 = 0. \tag{87}$$

The solution to this equation is simply

$$\mathcal{M}_9(s) = \mathcal{M}_9(0)\mathrm{e}^{-\ell_9 s}, \qquad \ell_9 \equiv \omega_{0|4} + 4\omega_{0|2}\gamma(\widetilde{a}). \tag{88}$$

Since $\omega_{0|4} > 0$ [44], one has $\ell_9 > 0$ and so $\mathcal{M}_9$ decays to 0.

The remaining eight moments in (85) are coupled. In matrix form, equation (69) becomes

$$(\delta_{\sigma\sigma'}\partial_s + \mathcal{L}_{\sigma\sigma'})\mathcal{M}_{\sigma'} = \mathcal{C}_\sigma, \qquad \sigma = 1, \ldots, 8. \tag{89}$$

Here, $\boldsymbol{\mathcal{M}}$ is a vector made of the following 8 moments

$$\boldsymbol{\mathcal{M}} = \begin{pmatrix} M^*_{4|0} \\ M^*_{2|xx} \\ M^*_{2|yy} \\ M^*_{0|yyyy} \\ M^*_{0|zzzz} \\ M^*_{2|xy} \\ M^*_{0|xxxy} \\ M^*_{0|xyyy} \end{pmatrix}, \tag{90}$$

and the square matrix $\boldsymbol{\mathcal{L}}$ is

$$\boldsymbol{\mathcal{L}} = 4\omega_{0|2}\gamma(\widetilde{a})\boldsymbol{\mathcal{I}} + \boldsymbol{\mathcal{L}}', \tag{91}$$

where $\boldsymbol{\mathcal{I}}$ is the 8×8 identity matrix and

$$\boldsymbol{\mathcal{L}}' = \begin{pmatrix} \omega_{4|0} & 0 & 0 & 0 & 0 & 4a^* & 0 & 0 \\ 0 & \omega_{2|2} & 0 & 0 & 0 & \frac{32}{21}a^* & 2a^* & 0 \\ 0 & 0 & \omega_{2|2} & 0 & 0 & -\frac{10}{21}a^* & 0 & 2a^* \\ 0 & 0 & 0 & \omega_{0|4} & 0 & -\frac{96}{245}a^* & 0 & -\frac{12}{7}a^* \\ 0 & 0 & 0 & 0 & \omega_{0|4} & \frac{24}{245}a^* & \frac{12}{7}a^* & \frac{12}{7}a^* \\ \frac{7}{15}a^* & \frac{2}{7}a^* & \frac{9}{7}a^* & -\frac{7}{3}a^* & -\frac{1}{3}a^* & \omega_{2|2} & 0 & 0 \\ 0 & \frac{15}{49}a^* & -\frac{6}{49}a^* & -\frac{5}{2}a^* & -\frac{5}{14}a^* & 0 & \omega_{0|4} & 0 \\ 0 & -\frac{6}{49}a^* & \frac{15}{49}a^* & 2a^* & \frac{1}{7}a^* & 0 & 0 & \omega_{0|4} \end{pmatrix}. \tag{92}$$

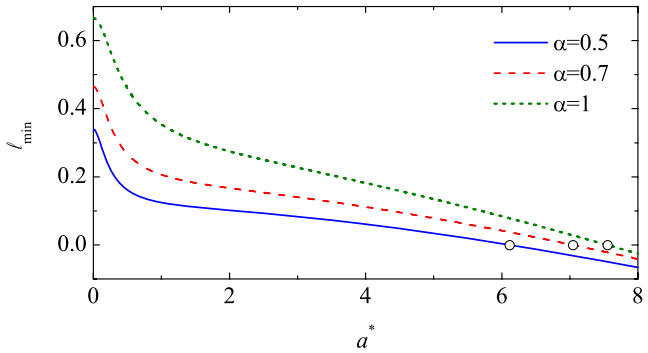

Figure 5. Plot of the smallest eigenvalue, $\ell_{\min}$, associated with the time evolution of the symmetric fourth-degree moments as a function of a^* for $\alpha = 0.5$ (solid line), $\alpha = 0.7$ (dashed line), and $\alpha = 1$ (dotted line). The circles indicate the location of the corresponding values of the critical shear rate.

In addition, $\boldsymbol{\mathcal{C}}$ is a vector of elements made of second-degree moments, namely

$$\mathcal{C}_1 = \tfrac{9}{4}\lambda_1^* - \lambda_2^*\left(M_{0|xx}^{*\,2} + M_{0|yy}^{*\,2} + M_{0|zz}^{*\,2} + 2M_{0|xy}^{*\,2}\right), \tag{93}$$

$$\mathcal{C}_2 = \tfrac{3}{2}\lambda_3^* M_{0|xx}^* - \tfrac{1}{3}\lambda_4^*\left(2M_{0|xx}^{*\,2} - M_{0|yy}^{*\,2} - M_{0|zz}^{*\,2} + M_{0|xy}^{*\,2}\right), \tag{94}$$

$$\mathcal{C}_3 = \tfrac{3}{2}\lambda_3^* M_{0|yy}^* - \tfrac{1}{3}\lambda_4^*\left(2M_{0|yy}^{*\,2} - M_{0|xx}^{*\,2} - M_{0|zz}^{*\,2} + M_{0|xy}^{*\,2}\right), \tag{95}$$

$$\mathcal{C}_4 = \tfrac{1}{35}\lambda_5^*\left(51M_{0|yy}^{*\,2} + 6M_{0|xx}^{*\,2} + 6M_{0|zz}^{*\,2} - 48M_{0|xy}^{*\,2}\right), \tag{96}$$

$$\mathcal{C}_5 = \tfrac{1}{35}\lambda_5^*\left(51M_{0|zz}^{*\,2} + 6M_{0|xx}^{*\,2} + 6M_{0|yy}^{*\,2} + 12M_{0|xy}^{*\,2}\right), \tag{97}$$

$$\mathcal{C}_6 = \tfrac{3}{2}\lambda_3^* M_{0|xy}^* - \lambda_4^* M_{0|xy}^*\left(M_{0|xx}^* + M_{0|yy}^*\right), \tag{98}$$

$$\mathcal{C}_7 = \tfrac{3}{7}\lambda_5^* M_{0|xy}^*\left(5M_{0|xx}^* - 2M_{0|yy}^*\right), \tag{99}$$

$$\mathcal{C}_8 = \tfrac{3}{7}\lambda_5^* M_{0|xy}^*\left(5M_{0|yy}^* - 2M_{0|xx}^*\right). \tag{100}$$

The solution of equation (89) can be written as

$$\boldsymbol{\mathcal{M}}(s) = \mathrm{e}^{-\boldsymbol{\mathcal{L}}s}\cdot[\boldsymbol{\mathcal{M}}(0) - \boldsymbol{\mathcal{M}}_\infty] + \boldsymbol{\mathcal{M}}_\infty, \tag{101}$$

where

$$\boldsymbol{\mathcal{M}}_\infty = \boldsymbol{\mathcal{L}}^{-1}\cdot\boldsymbol{\mathcal{C}}. \tag{102}$$

Similarly to the cases discussed above, the long time behavior of $\mathcal{M}_\sigma$ ($\sigma = 1, \ldots, 8$) is governed by the eigenvalue $\ell_{\min}$ of the matrix $\boldsymbol{\mathcal{L}}$ with the smallest real part. We have checked that $\ell_{\min}$ is a real quantity that, for a given value of α, monotonically decreases with increasing shear rate. It is plotted in figure 5 for $\alpha = 0.5$, 0.7, and 1. The most important feature of figure 5 is that, for any given value of α, $\ell_{\min}$ becomes negative for

J. Stat. Mech. (2007) P08021

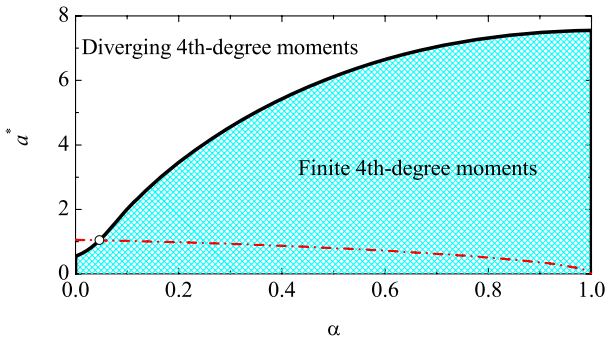

Figure 6. Phase diagram for the asymptotic long time behavior of the fourth-degree (symmetric) moments. The shaded region below the curve $a_c^*(\alpha)$ (thick solid line) corresponds to states with finite asymptotic values of the scaled fourth-degree moments, while the region above the curve defines the states where those moments diverge in time. The dash–dotted line represents the steady-state points $a_s^*(\alpha)$. It intercepts the critical curve $a_c^*(\alpha)$ at the point $(\alpha, a^*) = (0.046, 1.041)$.

shear rates larger than a certain 'critical' value $a_c^*(\alpha)$. This means that, if $a^* > a_c^*$, the symmetric fourth-degree moments exponentially grow in time. This singular behavior of the scaled moments implies that the velocity distribution function (scaled with the thermal speed) develops an algebraic high velocity tail in the long time limit. It is interesting to remark that this effect is also present in the elastic limit, where it has been extensively studied [47]–[49]. As observed in figure 5, the main influence of inelasticity is to decrease the value of the critical shear rate.

Let us analyze the phase diagram associated with the singular behavior of the fourth-degree moments. This is shown in figure 6, where the curve $a_c^*(\alpha)$ splits the parameter space into two regions: the region below the curve corresponds to states (α, a^*) with finite asymptotic values of the scaled fourth-degree moments (i.e., $\ell_{\min} > 0$), while the region above the curve defines the states where those moments diverge in time ($\ell_{\min} < 0$). Figure 6 also includes the locus of steady-state points (α, a_s^*) (cf equation (67)). Below the latter curve the inelastic cooling dominates over the viscous heating and so the temperature decreases in time, while the opposite happens above it. It is apparent that the curve $a_s^*(\alpha)$ lies inside the region $a^* < a_c^*(\alpha)$, except for the small interval $\alpha \leq 0.046$ or, equivalently, $a_s^*(0.046) = 1.041 \leq a^* \leq a_s^*(0) = 1.054$. In conclusion, in order to find diverging moments, one has to consider states with rather large values of the shear rate at which the viscous heating is much higher than the collisional cooling.

For states with $a^* < a_c^*(\alpha)$ the scaled (symmetric) fourth-degree moments reach well-defined finite values in the asymptotic long time limit. From equation (101) one has

$$\lim_{s\to\infty} \boldsymbol{\mathcal{M}}(s) = \boldsymbol{\mathcal{M}}_\infty, \tag{103}$$

where $\boldsymbol{\mathcal{M}}_\infty$ is defined by equation (102). As an illustration, figure 7 shows the shear-rate dependence of the asymptotic long time values of $M_{4|0}^* = (nv_0^4)^{-1} \int d\mathbf{V} V^4 f(\mathbf{V})$ for $\alpha = 0.5$, 0.7, and 1. The values of $M_{4|0}^*$ at $a^* = 0$ correspond to the homogeneous cooling state [44]. We observe that, given a value of α, the scaled moment $M_{4|0}^*$ rapidly increases

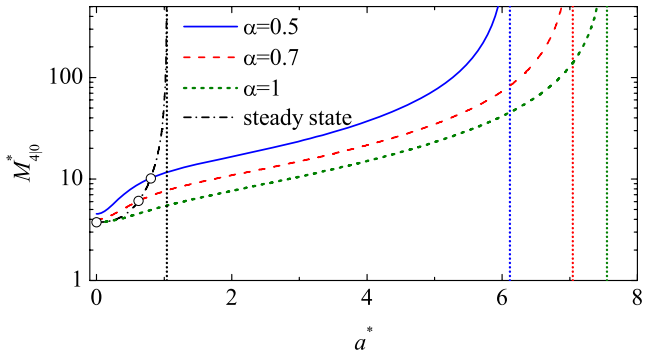

Figure 7. Plot of the asymptotic long time value of the scaled moment $M^*_{4|0}$ as a function of a^* for $\alpha = 0.5$ (solid line), $\alpha = 0.7$ (dashed line), and $\alpha = 1$ (dotted line). The dash–dotted line represents the values of $M^*_{4|0}$ at the steady states $a^*_s(\alpha)$ for $0.046 < \alpha \leq 1$. It intercepts the curves representing $M^*_{4|0}(a^*)$ at the points indicated by circles. The vertical dotted lines are the asymptotes of the curves.

with the shear rate, having a vertical asymptote at $a^* = a^*_c(\alpha)$. Moreover, for a given value of a^*, the value of the moment increases with dissipation. Figure 7 also includes the curve representing the values of $M^*_{4|0}$ at the steady states $a^*_s(\alpha)$. This curve has a vertical asymptote at $a^* = 1.041$.

5. Concluding remarks

The simple or uniform shear flow is perhaps the most widely studied inhomogeneous state for elastic and inelastic gases. Despite its apparent simplicity, this state has proven to be useful to shed light on the non-linear response of the system to the presence of strong shearing. This response is conventionally measured by the non-Newtonian rheological properties (namely, the non-linear shear viscosity η^* and viscometric function Ψ), which are related to the second-degree velocity moments (pressure tensor). On the other hand, higher degree moments are also important to provide indirect information on the features of the velocity distribution function. For inelastic gases, there are two relevant control parameters: the shear rate a scaled with an effective collision frequency ν_0, i.e., the reduced shear rate $a^* = a/\nu_0$, and the coefficient of normal restitution α. When the velocity moments are conveniently scaled with the thermal speed, they are expected to become, after a kinetic transient regime, non-linear functions of both control parameters.

To address the above issues in the context of the Boltzmann equation without having to resort to approximate methods or computer simulations, one can consider simplified collision models. As in the case of elastic collisions [47], the inelastic Maxwell model (IMM) renders itself to an analytical treatment. Here, taking advantage of a recent derivation by the authors of the collisional moments for IMM through the fourth degree [44], we have determined the pressure tensor and the fourth-degree velocity moments of the USF problem in an exact way. Two different classes of IMM have been defined: Model A, where ν_0 is independent of temperature, and Model B, where ν_0 is an increasing function of temperature. In the USF the temperature changes in time due to two opposite effects:

J. Stat. Mech. (2007) P08021

viscous heating and collisional cooling. Therefore, a steady state is eventually achieved in Model B when both effects cancel each other. However, in Model A a steady state does not generally exist, except for a specific value $a^* = a_s^*(\alpha)$, equation (67). It is important to note that the results in the steady state are the same for both classes of models. Since the reduced shear rate a^* changes with time in Model B, the goal of obtaining the velocity moments as functions of a^* and α requires the use of numerical tools in that case. However, $a^* = \text{const}$ in Model A and so the independent influence of a^* and α can be studied analytically. Thus, in this paper we have focused on Model A, except in what concerns the steady state which, as said before, is common to Models A and B.

As mentioned above, the relevant transport properties in the USF problem are the non-linear shear viscosity $\eta^*(a^*)$ and the viscometric function $\Psi(a^*)$. Their explicit forms are given by equations (61) and (62), respectively. These results extend to inelastic collisions the expressions obtained long time ago by Ikenberry and Truesdell for (elastic) Maxwell molecules [51]. With respect to the dependence of $\eta^*(a^*)$ and $\Psi(a^*)$ on inelasticity, our results show that its influence is quite significant for small and moderate shear rates, both rheological properties being practically insensitive to dissipation in the region of high shear rates. In the steady-state solution, η_s^* and Ψ_s decrease when decreasing the coefficient of restitution. Moreover, as expected, the (scaled) third- and asymmetric fourth-degree moments vanish in the long time limit. Consequently, beyond the rheological properties, the next non-trivial moments are the symmetric fourth-degree moments. An important result is that, for a given value of the coefficient of restitution, these moments are divergent for shear rates larger than a certain critical value $a_c^*(\alpha)$. This singular behavior is also present in elastic systems [47]–[49], where it has been shown that this divergence is consistent with an algebraic high velocity tail of the velocity distribution function. The main effect of inelasticity is to decrease the value of $a_c^*(\alpha)$ as the gas becomes more inelastic. In addition, the phase diagram associated with this singular behavior shows that the value of $a_c^*(\alpha)$ is rather large in the whole domain $0 < \alpha \leq 1$, so that in order to get diverging moments one has to consider states at which the collisional cooling is strongly dominated by the viscous heating effect. As a consequence, non-linear shearing effects are still significant for $a^* < a_c^*$, as illustrated in figure 7 for the scaled moment $M_{4|0}^*$.

The results derived in this paper can be useful for analyzing different situations. First, the knowledge of the shear-rate dependence of the second- and fourth-degree moments of the USF allows one to determine the generalized transport coefficients characterizing transport around the simple shear flow [46]. Another possible direction of study is the extension of the present analysis for the rheological properties to multicomponent systems. Previous works carried out for IMM [37, 39] have shown the tractability of the Maxwell kinetic theory for these complex systems and stimulate the performance of this study in the near future.

Acknowledgments

Partial support from the Ministerio de Educación y Ciencia (Spain) through Grant No. FIS2007–60977 (partially financed by FEDER funds) and from the Junta de Extremadura through Grant No. GRU07046 is acknowledged.

J. Stat. Mech. (2007) P08021

References

[1] Campbell C S, 1990 *Annu. Rev. Fluid Mech.* **22** 57
[2] Goldhirsch I, 2003 *Annu. Rev. Fluid Mech.* **35** 267
[3] Santos A, Garzó V and Dufty J W, 2004 *Phys. Rev.* E **69** 061303
[4] Astillero A and Santos A, 2007 *Europhys. Lett.* **78** 24002
[5] Brilliantov N and Pöschel T, 2004 *Kinetic Theory of Granular Gases* (Oxford: Clarendon)
[6] Lun C K K, Savage S B, Jeffrey D J and Chepurniy N, 1984 *J. Fluid Mech.* **140** 223
[7] Jenkins J T and Richman M W, 1985 *Phys. Fluids* **28** 3485
[8] Jenkins J T and Richman M W, 1988 *J. Fluid Mech.* **192** 313
[9] Lun C K K and Bent A A, 1994 *J. Fluid Mech.* **258** 335
[10] Sela N, Goldhirsch I and Noskowicz S H, 1997 *Phys. Fluids* **8** 2337
[11] Brey J J, Ruiz-Montero M J and Moreno F, 1997 *Phys. Rev.* E **55** 2846
[12] Chou C-S and Richman M W, 1998 *Physica* A **259** 430
Chou C-S, 2000 *Physica* A **287** 127
Chou C-S, 2001 *Physica* A **290** 341
[13] Montanero J M, Garzó V, Santos A and Brey J J, 1999 *J. Fluid Mech.* **389** 391
[14] Montanero J M and Garzó V, 2002 *Physica* A **310** 17
[15] Lutsko J F, 2004 *Phys. Rev.* E **70** 061101
[16] Lutsko J F, 2006 *Phys. Rev.* E **73** 021302
[17] Garzó V, 2006 *Phys. Rev.* E **73** 021304
[18] Bobylev A V, Carrillo J A and Gamba I M, 2000 *J. Stat. Phys.* **98** 743
[19] Carrillo J A, Cercignani C and Gamba I M, 2000 *Phys. Rev.* E **62** 7700
[20] Ben-Naim E and Krapivsky P L, 2000 *Phys. Rev.* E **61** R5
[21] Cercignani C, 2001 *J. Stat. Phys.* **102** 1407
[22] Ernst M H and Brito R, 2002 *Europhys. Lett.* **58** 182
[23] Ernst M H and Brito R, 2002 *J. Stat. Phys.* **109** 407
[24] Ernst M H and Brito R, 2002 *Phys. Rev.* E **65** 040301(R)
[25] Baldasarri A, Marconi U M B and Puglisi A, 2002 *Europhys. Lett.* **58** 14
[26] Ben-Naim E and Krapivsky P L, 2002 *Phys. Rev.* E **66** 011309
[27] Krapivsky P L and Ben-Naim E, 2002 *J. Phys. A: Math. Gen.* **35** L147
[28] Ben-Naim E and Krapivsky P L, 2002 *Eur. Phys. J.* E **8** 507
[29] Bobylev A V and Cercignani C, 2002 *J. Stat. Phys.* **106** 547
[30] Marconi U M B and Puglisi A, 2002 *Phys. Rev.* E **65** 051305
[31] Marconi U M B and Puglisi A, 2002 *Phys. Rev.* E **66** 011301
[32] Bobylev A V and Cercignani C, 2003 *J. Stat. Phys.* **110** 333
[33] Bobylev A V, Cercignani C and Toscani G, 2003 *J. Stat. Phys.* **111** 403
[34] Santos A and Ernst M H, 2003 *Phys. Rev.* E **68** 011305
[35] Santos A, 2003 *Physica* A **321** 442
[36] Ben-Naim E and Krapivsky P L, 2003 *Granular Gas Dynamics* (*Lecture Notes in Physics* vol 624) ed T Pöschel and N Brilliantov (Berlin: Springer) pp 65–93
[37] Garzó V, 2003 *J. Stat. Phys.* **112** 657
[38] Brito R and Ernst M H, 2004 *Advances in Condensed Matter and Statistical Mechanics* ed E Korutcheva and R Cuerno (New York: Nova Science) pp 177–202
[39] Garzó V and Astillero A, 2005 *J. Stat. Phys.* **118** 935
[40] Bobylev A V and Gamba I M, 2006 *J. Stat. Phys.* **124** 497
[41] Ernst M H, Trizac E and Barrat A, 2006 *J. Stat. Phys.* **124** 549
[42] Barrat A, Trizac E and Ernst M H, 2007 *J. Phys. A: Math. Theor.* **40** 4057
[43] Santos A, 2007 *Rarefied Gas Dynamics* vol 25, ed A K Rebrov and I S Ivanov, at press [cond-mat/0608627]
[44] Garzó V and Santos A, 2007 *Preprint* cond-mat/0703704
[45] Kohlstedt K, Snezhko A, Sapozhnikov M V, Arnarson I S, Olafsen J S and Ben-Naim E, 2005 *Phys. Rev. Lett.* **95** 068001
[46] Garzó V, 2007 *J. Phys. A: Math. Theor.* at press [0705.0092]
[47] Garzó V and Santos A, 2003 *Kinetic Theory of Gases in Shear Flows. Nonlinear Transport* (Dordrecht: Kluwer–Academic)
[48] Santos A, Garzó V, Brey J J and Dufty J W, 1994 *Phys. Rev. Lett.* **71** 3971
Santos A, Garzó V, Brey J J and Dufty J W, 1994 *Phys. Rev. Lett.* **72** 1392 (erratum)
[49] Santos A and Garzó V, 1995 *Physica* A **213** 409

J. Stat. Mech. (2007) P08021

[50] Truesdell C and Muncaster R G, 1980 *Fundamentals of Maxwell's Kinetic Theory of a Simple Monatomic Gas* (New York: Academic)
[51] Ikenberry E and Truesdell C, 1956 *J. Ration. Mech. Anal.* **5** 1
Truesdell C, 1956 *J. Ration. Mech. Anal.* **5** 55
[52] Chapman S and Cowling T G, 1970 *The Mathematical Theory of Nonuniform Gases* (Cambridge: Cambridge University Press)
[53] Lees A W and Edwards S F, 1972 *J. Phys. C: Solid State Phys.* **5** 1921
[54] Tij M, Tahiri E E, Montanero J M, Garzó V, Santos A and Dufty J W, 2001 *J. Stat. Phys.* **103** 1035

J. Stat. Mech. (2007) P08021